Cryogenics 128 (2022) 103585

Contents lists available at ScienceDirect

Cryogenics

journal homepage: www.elsevier.com/locate/cryogenics

An active convective ^{4}He heat switch

Andrew J. May [a,b,c], Susanna Azzoni [a,d], Simon Melhuish [a], Lucio Piccirillo [a], Daniel Seal [a,c,e], Thomas Sweetnam [a], Joseph Winnicki [a]

[a] Jodrell Bank Centre for Astrophysics, School of Physics and Astronomy, University of Manchester, Oxford Road, Manchester M13 9PL, UK
[b] RF and Cryogenics Group, Accelerator Science and Technology Centre, STFC, Daresbury Laboratory, Daresbury WA4 4AD, UK
[c] Cockcroft Institute, Daresbury Laboratory, Daresbury WA4 4AD, UK
[d] Department of Physics, University of Oxford, Denys Wilkinson Building, Keble Road, Oxford OX1 3RH, UK
[e] Engineering Department, Lancaster University, Lancaster LA1 4YR, UK

ARTICLE INFO

Keywords:
Heat switch
Thermal switch
Convection
^{4}He
Active switch

ABSTRACT

The design and experimental demonstration are reported of an active convective heat switch suitable for use at cryogenic temperatures. The switch is mechanically simple, relatively inexpensive, and requires no moving parts, instead being operated entirely using heaters. The working gas used is ^{4}He in a closed cycle and, as such, the switch requires no external gas connections. Closed conductances on the order of 50 mW/K have been demonstrated with residual open conductances on the order of 0.4 mW/K. Novel modelling is presented which shows excellent agreement with the experimental data and significant improvement over existing models.

1. Background

Heat switches, of which there are many varieties, are used in a range of cryogenic systems to make and break thermal connections as required.

Switches may be categorised primarily by the method of changing the conductance through the switch (e.g., mechanical, gas-gap, liquid-gap, superconducting, magnetoresistive, etc.) and secondarily by the method of actuation (i.e., active or passive, depending on whether the open/closed state is set by an external control signal or by the temperature of the switch respectively).

The salient figures of merit for a given switch are the open conductance, closed conductance, ratio of these two values, and time required to change between states.

We report here a novel active convective heat switch using ^{4}He as the working fluid.

2. Design

The forthcoming generation of Cosmic Microwave Background observatories will be based around large cryogenic receivers housing multiple cold optics stages at progressively lower temperatures down to <1 K; typically, 40 K and 4 K stages are cooled using pulse-tube cryocoolers, with either closed cycle ^{4}He/^{3}He sorption coolers or a dilution refrigerator providing <1 K stages (see for example References [1,2]). Due to the large masses and high level of thermal isolation of the <1 K cold stages, modelled cooldown times can be on the order of 1 month in the absence of any explicit precooling schemes [3]; these durations can be significantly reduced through the use of heat switches [4]. The <1 K cold stages may be strongly coupled to the 4 K stage to precool close to 4 K, then decoupled to be cooled further to <1 K. A second application of heat switches in these types of receivers is the operation of the cryopumps required to operate sorption coolers which must also be coupled and decoupled from the 4 K stage during operation [4].

The active convective switch described here has been developed for both applications. It is clear that the switch closed conductance should be maximised for effective heat transfer and the open conductance minimised to reduce the thermal load on the cold stage. Times for the transition between these two states on the order of a few minutes are acceptable.

The switch design that has been developed essentially consists of a circuit comprising two stainless steel tubes (having relatively low thermal conductance, measuring 0.25 in x 0.010 in x 94 mm) and a copper heat exchanger (having relatively high thermal conductance) at either end connected to the thermal stages that one wishes to couple and decouple. The switch is charged with helium gas at room temperature and permanently sealed. The key novelty in the design of this switch is the addition of a charcoal cryopump which may be used to evacuate or fill the circuit with helium, opening and closing the switch respectively (i.e., providing the active control). A cut-away schematic of the switch is

E-mail address: andrew.may@stfc.ac.uk (A.J. May).

https://doi.org/10.1016/j.cryogenics.2022.103585
Received 1 July 2022; Received in revised form 23 September 2022; Accepted 9 October 2022
Available online 20 October 2022

shown in Fig. 1 and photograph of a completed switch in Fig. 2.

The cryopump is weakly coupled to the cryostat 4 K stage and has a small resistive heater attached. When the heater is off, the pump will be cooled to ~4 K, at which temperature the charcoal will strongly physically adsorb the helium [5], removing it from the circuit. In this state, the only mechanism by which heat may pass through the switch is conduction through the thin-walled stainless steel tubes. Owing to the relatively low thermal conductivity of stainless steel at cryogenic temperatures and the small cross-sectional area of the tubes, the heat flow in this condition is minimal. This is the open state of the switch, whereby the two ends of the switch (denoted "hot" and "cold" in Fig. 1) are decoupled.

In order to close the switch, the cryopump is heated to ~40 K. At this temperature, the helium is only weakly adsorbed [5] and the circuit fills with gas. As long as the cryostat cold stages are designed so as to have the cold end positioned higher with respect to gravity than the hot end[1], a convective loop is established as shown in Fig. 1. This provides a very effective mechanism for heat transfer and hence a high conductance through the switch in the closed position. The gas entering the hot end warms as it passes through the heat exchanger. It then, having warmed and hence reduced in density, rises to the cold end. Here, heat is rejected as it passes through the cold heat exchanger, and the gas increases in density again, returning to the hot end. This operating mode is referred to as gas–gas. This operating mode was studied in detail via analytical modelling, computational fluid dynamics (CFD) modelling, and experimental measurements as reported in Sections 3–5 respectively.

A different flow pattern that was considered during this analysis was that where separate convective loops could be established within each tube. However, as discussed in Section 4, this type of flow pattern could not be reproduced in CFD. Furthermore, as discussed in 5, a single-tube switch showed "closed" conductance significantly lower than half that of a double-tube switch, constituting further evidence in favour of the flow pattern described above. Finally, Torii and Maris [6] make reference to negligible convection within a tube with diameters < 10 mm (diameter of the tubes used here is 6.35 mm (0.25 in.)).

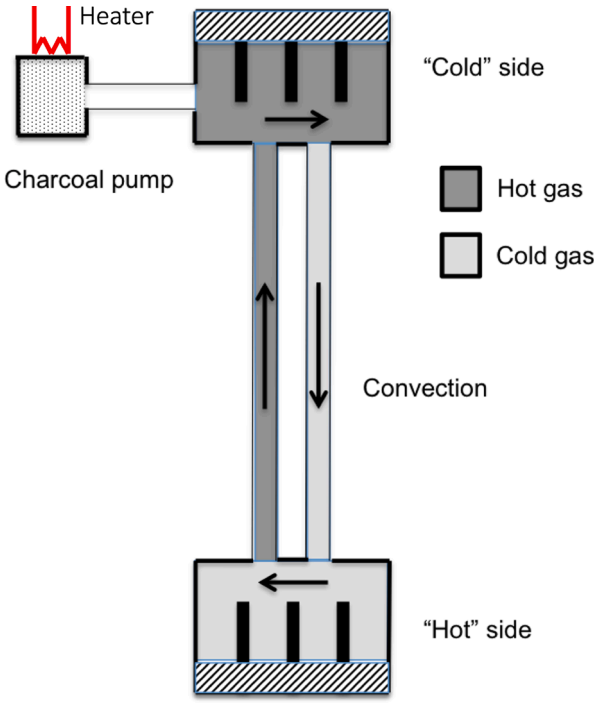

Fig. 1. Convective heat switch schematic.

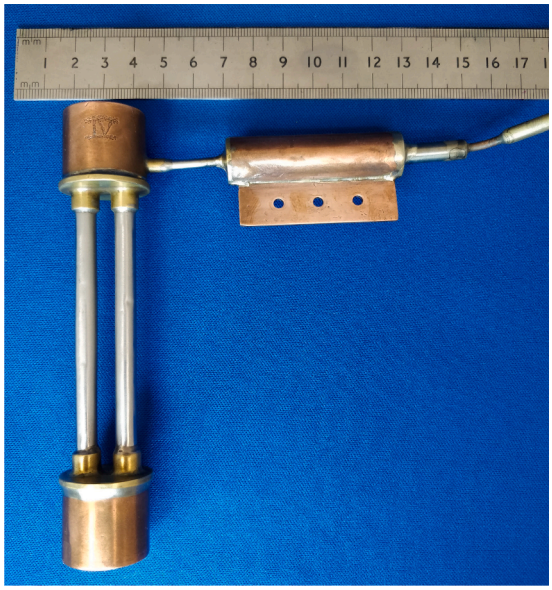

Fig. 2. Photograph of convective heat switch built in Manchester.

It is also expected that there exists a second regime of operation whereby the cold end is suitably low in temperature that the helium condenses to liquid in the heat exchanger, falls under the action of gravity to the hot end where it evaporates and returns as low density gas to the cold end. This operating mode will be referred to as gas–liquid, and is not treated here. It is noted however that in the case of ^{4}He, the superfluid nature is such that below the lambda point a superfluid film will form on the inside walls of the tubes and be accelerated in the direction of positive temperature gradient until it is warmed above T_λ and the superfluid state is broken; this process is expected to contribute significantly to the heat transfer in the switch in this mode.

Furthermore, there is a third expected regime whereby both ends of the switch are suitably cold to condense liquid. In this case, the lower vapour pressure in the cold heat exchanger serves to pump vapour off the liquid in the hot end which then rises to the cold end, recondenses at a lower temperature and then returns under the action of gravity as liquid. Again, this behaviour may be complicated by the superfluid nature of ^{4}He below T_λ where it is expected that a superfluid film would again form along the walls of the tubes moving towards the hot side and contributing to the transport of heat. Again, this is not reported on here. This operating mode is referred to as liquid–liquid.

Both gas–liquid and liquid–liquid modes are expected to be the subject of future work.

3. Analytical model

Having provided a qualitative understanding of this switch, we now consider a quantitative description of the gas–gas mode of operation. On the assumption that the gas is evacuated to an extent that any residual heat transfer through the gas is negligible[2], the heat flow $\dot{Q}_{open}$ in the open state may be calculated as a function of the two end temperatures T_H and T_C as

$$\dot{Q}_{open} = \frac{A}{L}\int_{T_C}^{T_H} k(T)dT \tag{1}$$

[1] This may be achieved with copper heat straps where the design does not naturally support this geometry

[2] This assumption is addressed experimentally in Section 5.2

where $k(T)$ is the conductivity of the steel, A is the total cross sectional area of the two tubes, and L is the length of the tubes between the heat exchangers.

The closed conductance on the other hand is somewhat more complex; an effective model is reported here extending the work of Torii and Maris [6].

It should be noted that the contribution from conduction through the steel remains, although ideally (in order to have a high switching ratio), this term will be dominated out by the contribution from the convective heat transfer.

Firstly, taking the continuity equation [7] and considering that in equilibrium the flow is steady, it may be seen that the quantity ρUA is constant for any "cut" through the circuit shown in Fig. 1, where ρ is the gas density, U is the mean flow velocity and A is the cross sectional area of the flow.

Next, it is assumed that heat transfer between the gas and solid components of the switch only occurs at the two heat exchangers. The gas can therefore be considered to exist in two discrete regimes, also shown in Fig. 1.

The next step is to consider that in the equilibrium condition, the sum of potentials around the loop is zero, i.e., the total pressure gain around the circuit has to be equal to the total pressure loss in order that the equilibrium condition is satisfied. The source of pressure rise is the buoyancy force; this occurs as the switch supports a denser (colder) gas at the top of the switch and a less dense (warmer) gas at the bottom, with respect to gravity. The pressure gain ΔP_ρ may be found from the difference in densities as

$$\Delta P_\rho = \Delta\rho g z = (\rho_1 - \rho_2) g z \tag{2}$$

where g is the acceleration due to gravity and z is the vertical distance with respect to gravity between the heat exchangers.

In opposition to this are pressure losses in the flow due to dissipative forces; viscous effects in the flow as it travels around the loop causes a drop in pressure. In the case of laminar flow[3], the pressure drop per unit length of tube travelled L is given for this geometry by the Darcy–Weisbach equation [7] as

$$\frac{\Delta P_\mu}{L} = \frac{128 \mu Q}{\pi D^4} \tag{3}$$

where μ is the dynamic viscosity of the fluid, Q is the volumetric flow rate and D tube diameter.

Considering the two flow regimes shown in Fig. 1, the sum of the viscous losses around the circuit is given by

$$\Delta P_{\mu,1} + \Delta P_{\mu,2} = \left(\frac{128 \mu Q L}{\pi D^4}\right)_1 + \left(\frac{128 \mu Q L}{\pi D^4}\right)_2 \tag{4}$$

By considering that the volumetric flow is related to mass flow $\dot{M}$ (which, from continuity, we know to be constant around the circuit) by

$$Q = \frac{\dot{M}}{\rho} \tag{5}$$

and taking the lengths of the two sections to be the same, i.e.,

$$L_1 = L_2 \tag{6}$$

and defining L_0 to be the total length of the circuit, i.e.,

$$L_0 \equiv L_1 + L_2 \tag{7}$$

then it follows that the sum of the viscous losses can be rewritten as

$$\Delta P_{\mu,1} + \Delta P_{\mu,2} = \frac{8 \dot{M} L_0}{\pi r^4} \cdot \left(\frac{\mu_1}{\rho_1} + \frac{\mu_2}{\rho_2}\right) = \Delta P_\mu \tag{8}$$

Recalling that the sum of potentials around the loop is zero gives

$$(\rho_1 - \rho_2) g z = \frac{4 \dot{M} L_0}{\pi r^4} \cdot \left(\frac{\mu_1}{\rho_1} + \frac{\mu_2}{\rho_2}\right) \tag{9}$$

Rearranging for the mass flow rate gives

$$\dot{M} = \frac{\pi r^4}{4 L_0} \cdot \frac{(\rho_1 - \rho_2) g z}{\frac{\mu_1}{\rho_1} + \frac{\mu_2}{\rho_2}} \tag{10}$$

This analysis is thus far consistent with the approach taken by Torii and Maris [6]. We now develop the model further as follows.

By considering a control volume around each heat exchanger, the first law gives that, in the steady state condition, the heat transferred into/out of the switch is equal to the difference in enthalpies of the outgoing and returning gas flows to the heat exchanger. Thus, the heat flow through the switch $\dot{Q}$ is the product of the mass flow (constant around the circuit) and the difference in enthalpies Δh. This gives

$$\dot{Q} = \dot{M} \cdot \Delta h = \frac{\pi r^4}{4 L_0} \cdot \frac{(\rho_1 - \rho_2) g z}{\frac{\mu_1}{\rho_1} + \frac{\mu_2}{\rho_2}} \cdot (h_2 - h_1) \tag{11}$$

It may further be seen that the difference in enthalpy (neglecting pressure loss through the heat exchanger due to the short path length) is

$$h_2 - h_1 = c_p (T_2 - T_1) \tag{12}$$

where c_p is the specific heat capacity at constant pressure. It is important to note in designing this type of switch that the heat exchangers will in reality be imperfect; the exit temperature of the flow will approach but not be equal to the heat exchanger sink temperature, i.e., $T_1 > T_C$ and $T_2 < T_H$.

From Eq. 11, it can be seen that in order to find the power through the switch the densities and temperatures of the two regimes must be determined. The densities are a function of temperatures themselves, as well as the initial gas charge in the switch. It is clear from inspection that the higher the charge of gas in the switch, the greater the closed conductance of the switch. However, the practical upper limit on the charge is given by either the capacity of the cryopump (as it must be able to fully evacuate the circuit) or the mechanical limitation given by the structure in terms of the allowable charging pressure at room temperature, whichever is the lower. The cryopump may be easily sized greater than this and hence in practice the switch mechanical limitation is likely to be the determining factor. This is typically found using a finite element approach where a limit greater than 30 bar at room temperature is not unreasonable.

Given the switch geometry and the initial charging pressure, the number of moles of gas may be calculated from the perfect gas law. By considering the two gas regimes, the number of moles and hence the density may be calculated as a function of the two regime temperatures.

Using the model described by Eq. 10, it may seen how a contour plot may be produced for the mass flow through the switch as a function of the two regime temperatures as given in Fig. 3. As Eq. 10 shows this scaling with r^4 and L_0^{-1}, the plot is presented in arbitrary units.

Furthermore, it can be seen from Eq. 11 how this translates into the power through the switch as a function of the two regime temperatures as shown in Fig. 4.

It is clear from Fig. 4 that there exists a temperature regime supporting peak heat transfer. If the temperature differential is too great, then the density in the denser region will be sufficiently high so as to result in great enough viscous losses so as to more than offset the increased head gain from buoyancy forces.

Next, it is considered that the real values of mass flow and power will

[3] This assumption is addressed in Section 4

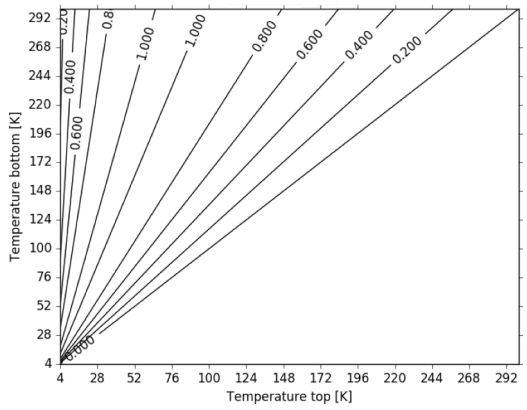

Fig. 3. Mass flow in switch (arbitrary units).

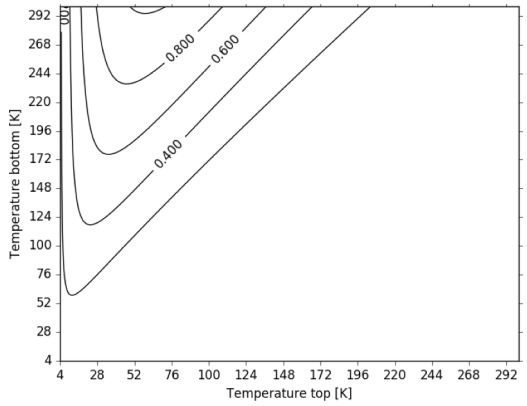

Fig. 4. Heat flow in switch (arbitrary units).

depend heavily on the efficiency of the heat exchangers. The heat exchanger geometries are identical and, as the mass flow through both is the same, the assumption is made that the efficiency of each is also the same. A model can then be considered where the efficiency of both exchangers is parameterized by a single value f as

$$T_2 = \left(\frac{T_H + T_C}{2}\right) + f\left(\frac{T_H - T_C}{2}\right) \tag{13}$$

$$T_1 = \left(\frac{T_H + T_C}{2}\right) - f\left(\frac{T_H - T_C}{2}\right) \tag{14}$$

such that where $f = 0$, the mean temperature $T_m = T_2 = T_1$, and where $f = 1, T_2 = T_H$ and $T_1 = T_C$. Unfortunately, modelling of f from first principles is exceptionally difficult owing to the complex geometries used to maximise the surface area and the flow conditions in this part of the circuit. As such, f must be fit to experimental data as reported in Section 5.3.

Section 2 described qualitatively other heat transfer modes involving gas–liquid phase changes. The vapour pressure of ^{4}He at 3 K is 2.405E4 Pa [8]; therefore for a switch charge of <23.7 bar at 295 K, no liquid will be condensed in the switch and it is guaranteed to be operating in the gas–gas regime.

4. Computational fluid dynamics modelling

In order to further investigate the flow behaviour inside the switch, a computational fluid dynamics (CFD) study was carried out. The 3D CAD model of the switch, shown in Fig. 5, was imported into Autodesk CFD 2019[4].

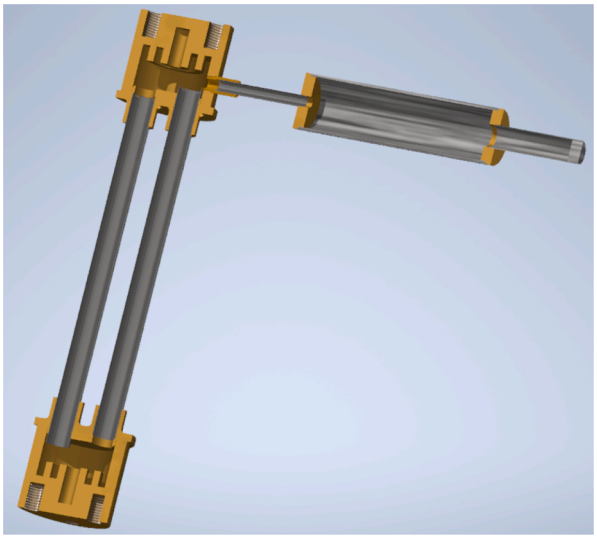

Fig. 5. Section-view of 3D CAD model of switch used for CFD model.

Material properties used for the simulations for OFHC copper, 304 stainless steel, and helium were taken from References [9–11]. The helium gas charge taken for the simulations was 335 mbar at 4 K (equivalent to 25 bar at room temperature).

Auto-meshing was used, giving a mesh length scale of 0.717 mm, with gap and surface refinement allowed. Further mesh refinement gave no difference in the final results. Turbulent flow was allowed by the model.

As a boundary condition, the cryopump housing temperature was set at 40 K (temperature typically operated to ensure desorption of helium gas). A series of simulations were then run with fixed heat loads applied at the switch warm end. For each simulation, the switch cold end temperature was set to the coldhead temperature given by the cryocooler load curve for the corresponding applied heat load at the switch warm end.

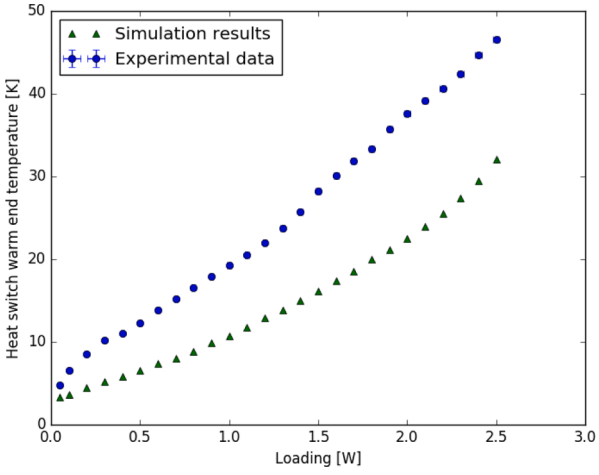

Fig. 6. Simulation results alongside experimental data for heat switch warm end temperature as a function of applied heat load (switch cold end at cryocooler temperature 4 K).

[4] autodesk.co.uk

In each case, the equilibrium warm end temperature was found for the applied heat load. Fig. 6 shows these data along side experimental data (see Section 5). Whilst the simulation appears to overestimate the overall conductance of the switch, the general form of the simulation results is consistent with that of the experimentally obtained data. It is suggested that this overestimation stems from difficulties in accurately capturing the turbulent flow in the heat exchangers.

Fig. 7 shows the temperature distribution in the gas. This appear to be consistent with that given by the model described in Section 3; i.e., of two discrete regimes as a result of heat transfer in the two heat exchangers dominating the gas dynamics. Similar conclusions can be drawn from the density distribution which follows the same form. The direction of flow shown in Figs. 7–9 arises from the assymmetry in the vertical position of the tubes as shown in Fig. 5.

Fig. 8 shows the gas velocity in the bottom heat exchanger. It can be seen from this that turbulent flow occurs in the heat exchanger as would be expected. It is the difficulty in capturing this and hence modelling the heat transfer between the copper and helium that is suggested to contribute to the discrepancy in Fig. 6.

Fig. 9 shows the gas velocity in the tubes. Laminar flow is clearly shown, consistent with the model described in Section 3 and use of the Darcy–Weisbach equation as described. This does highlight a limitation of the analytical model however, insofar as it doesn't account for turbulent pressure drops in the heat exchangers (although this is accounted for to some extent by the parameter f). The results in Fig. 9 are inconsistent with convection within a single tube, one of the flow models that was initially considered in Section 2.

5. Experimental testing

Along with the analytical and simulation work that was carried out and described in Sections 3 and 4, experimental measurements were made of the switch conductance in both the open and closed states.

Two experimental runs were carried out. The first run studied the change in switch conductance with gas charge (detailed below in Section 5.2); the second made detailed measurements of switch conductance with a fixed gas charge for comparison with the models described above (detailed in Section 5.3). In both runs, the same experimental setup was used.

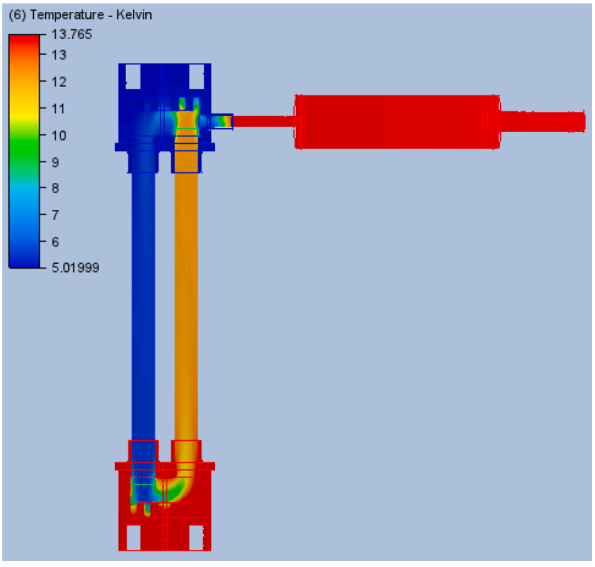

Fig. 7. Gas temperature distribution for simulation with 1.0 W applied heat load.

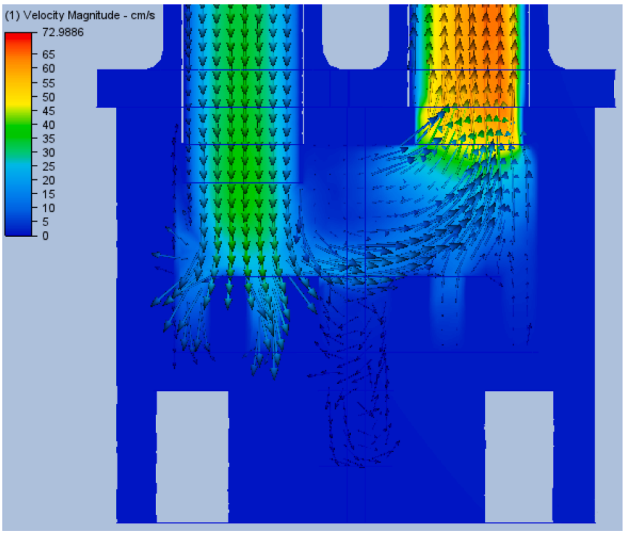

Fig. 8. Gas velocity distribution in bottom heat exchanger for simulation with 1.0 W applied heat load; colour indicates magnitude, arrows indicate direction.

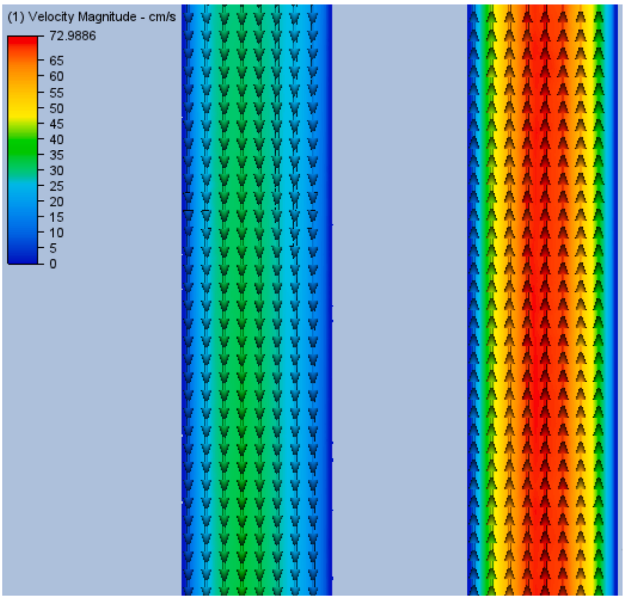

Fig. 9. Gas velocity distribution in the tubes for simulation with 1.0 W applied heat load; colour indicates magnitude, arrows indicate direction.

5.1. Experimental setup

In each run, a pair of switches (designated HS1 and HS2) were tested in a 4 K dry cryostat. The cold heat exchangers were mounted directly to the 4 K stage provided by a Sumitomo[5] RDK415D G-M cryocooler, as shown in Fig. 10. 330 Ω resistive heaters were mounted to the bottom heat exchangers to apply heat loads up to 3.1 W during testing. Heaters and diode thermometers were mounted to the switch cryopumps, which were weakly linked to the 4 K stage, to allow for temperature control and monitoring. Cernox[6] RTD thermometers were used to measure the temperatures of both heat exchangers.

Gas lines were soft-soldered to the charging connection at the end of each cryopump to allow the gas charge to be altered during cold testing.

[5] shicryogenics.com
[6] lakeshore.com

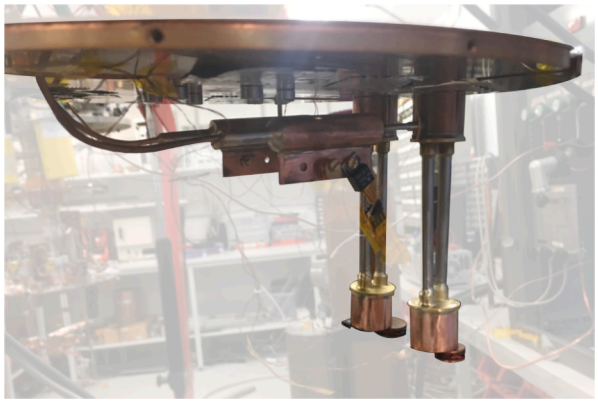

Fig. 10. Photograph of heat switches in test cryostat.

The switches were evacuated and the cryopumps baked out before cooldown. Each measurement set was automated using an XML script which applied incrementally increasing heat loads to the bottom heat exchanger, waited for an equilibrium to be reached, and then recorded the temperature at each end. At low powers, the cold end temperature was essentially constant, whereas at higher powers the cold end temperature increased according to the load curve profile of the cryocooler. The warm end temperature increased with power with the ΔT across the switch set in equilibrium by the switch conductance.

5.2. Switch conductance as a function of gas charge

It was expected a priori and from the model presented in Section 3 that the switch conductance would increase with gas charge. As discussed in Section 3, the practical upper limit on the charge is given by either the capacity of the cryopump (as it must be able to fully evacuate the circuit) or the mechanical limitation given by the structure in terms of the allowable charging pressure at room temperature, whichever is the lower. Finite element analysis for this particular switch showed that with an appropriate safety factor, a maximum room temperature charge of 30 bar was acceptable. The cryopump size allowed for a greater charge than this (charcoal capacity data taken from Pobell [5]), and so the first set of measurements were made of the open and closed switch conductance with room temperature equivalent (RTE) charges in 5 bar increments up to 30 bar.

Thermal conductivity $k(T)$ across a range of temperatures cannot typically be quantified by a single value. In the first instance however, to compare the relative performances for varying gas charges, the switches were characterised simply by plotting the measured temperature difference (ΔT) across the switch against the applied heat load and fitting a straight line to the data. This was done for both the closed and open states.

In the open state (i.e., with the cryopump cold and switch evacuated), no measurable difference was found between zero charge and each 5 bar increment up to and including 30 bar RTE charges. In all cases, (ΔT) was measured across the switch with power loadings up to 2.0 mW and with fitted gradients found of 0.4 mW/K. It is therefore concluded from the lack of increase at higher charges that there was no evidence of saturation, i.e., the cryopump capacity was sufficient to pump out at least a 30 bar RTE charge as expected from the calculations.

Fig. 11 shows the measured conductance in the closed state (i.e., with the pump at 40 K and the gas in the switch circuit) for charges between 0 and 30 bar. Again, the conductance is characterised simply by plotting the measured temperature difference (ΔT) across the switch against the applied heat load and fitting straight lines to the data.

Fig. 12 shows the linear approximations of conductances from Fig. 11 plotted directly as a function of RTE charge. It can be seen here that the closed switch conductance increases with the amount of helium,

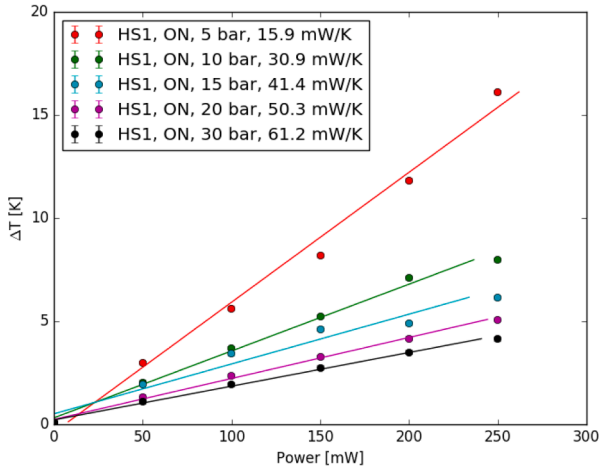

Fig. 11. Measured heat switch conductance in closed states for a range of RTE gas charges.

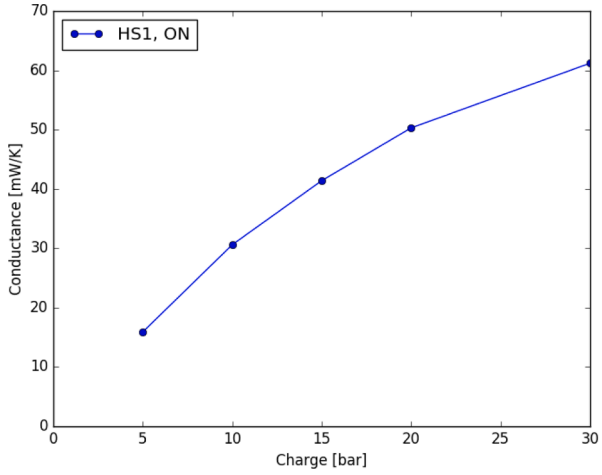

Fig. 12. Linear approximations of closed switch conductance as a function of RTE gas charges (line added to guide the eye).

however there are diminishing returns; extrapolating from this, it could be inferred that there exists some maximum charge beyond which there is no further improvement in closed conductance (notwithstanding the existing limitations on charge discussed above). At 30 bar RTE charge, the closed/open conductance ratio given by the linear approximations from these two data sets is 153.

5.3. Switch conductance as a function of temperature

Having investigated the dependence of switch conductance on RTE gas charge, the next experimental run was conducted to investigate the conductance as a function of temperature.

With the switch in the open state, incrementally increasing heat loads were applied to the warm end over a much wider range than in the data set given in the previous section. These data are shown in Fig. 13 along with modelled values using Eq. 1 and the same material properties referred to in Section 4. Reasonable agreement is shown between the experimental and modelled data. It is suggested that the cooling effect of the vapour inside the switch may contribute to the small discrepancy.

Fig. 14 shows the conductance measured in the closed state over a wide temperature range. It also shows the model described in Section 3 fit with the model from Torii and Maris [6] along with the new model proposed in this paper in Section 3 with $f = 0.25$.

It is clear to see the strong agreement between the new model and the

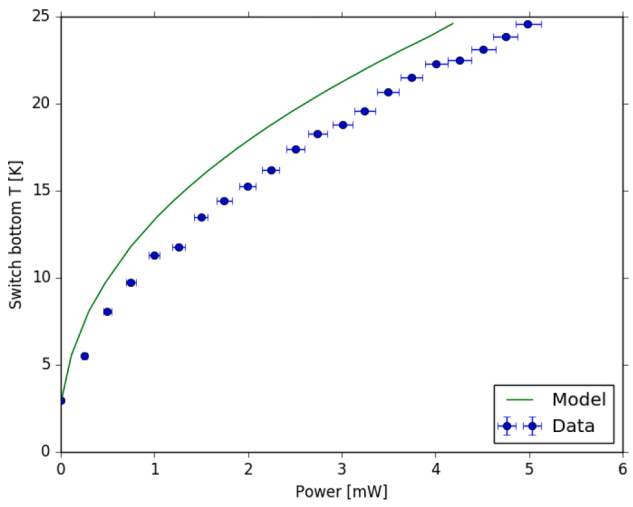

Fig. 13. Measured and calculated heat switch conductance in open state across wide temperature range.

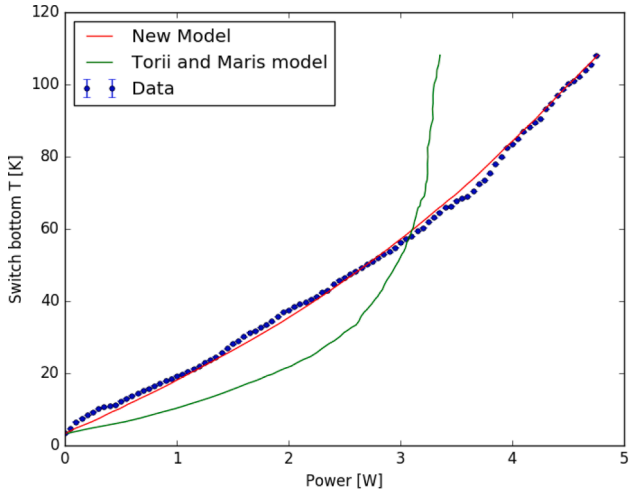

Fig. 14. Measured and modelled heat switch conductance in closed state across wide temperature range.

experimental data, as well as the divergence of the Torii-Maris model at high temperatures. This arises from the fact that the new model accounts for the temperature dependence of the viscosity μ of the helium gas, whereas the Torii-Maris model which only considered a small temperature range took μ to be constant. Across a wider temperature range, this assumption can no longer be considered valid as shown by Fig. 14. Also of note is the observation that the gradient of the experimental data and new model are close to constant over a wide temperature range, being on the order of 50 mW/K, consistent with the data in SubSection 5.3.

6. Conclusions

A novel cryopump-controlled convective heat switch has been designed for use at cryogenic temperatures. The design and experimental demonstration have been reported. Closed conductances on the order of 50 mW/K have been demonstrated with residual open conductances on the order of 0.4 mW/K. Novel modelling has presented which shows excellent agreement with the experimental data and significant improvement over existing models.

Declaration of Competing Interest

The authors declare that they have no known competing financial interests or personal relationships that could have appeared to influence the work reported in this paper.

Acknowledgements

The authors would like to thank the staff in the School of Physics and Astronomy Machine Shop at the University of Manchester for their exceptionally skilled machining of many of the parts described in this paper.

This work was supported by Science and Technology Facilities Council grant ST/L000768/1.

The authors would also like to thank Prof. H.J.M. ter Brake for helpful discussions on the various flow models described herein.

References

[1] Masi S, Battistelli E, de Bernardis P, Chapron C, Columbro F, Coppolecchia A, et al. Qubic V: Cryogenic system design and performance. J Cosmol Astropart Phys 2022; 2022:038.
[2] Galitzki N, Ali A, Arnold KS, Ashton PC, Austermann JE, Baccigalupi C, et al. The Simons Observatory: instrument overview. In: Millimeter, Submillimeter, and Far-Infrared Detectors and Instrumentation for Astronomy IX, 10708. International Society for Optics and Photonics. p. 1070804.
[3] Coppi G, Xu Z, Ali A, Galitzki N, Gallardo PA, May AJ, et al. Cooldown strategies and transient thermal simulations for the Simons Observatory. In: Millimeter, Submillimeter, and Far-Infrared Detectors and Instrumentation for Astronomy. IX, 10708. International Society for Optics and Photonics. p. 1070827.
[4] May A. Sub-Kelvin cryogenics for experimental cosmology, Ph.D. thesis, University of Manchester; 2019.
[5] Pobell F. Matter and methods at low temperatures. Springer Science & Business Media; 2007.
[6] Torii RH, Maris HJ. Low-temperature heat switch using unforced convection. Rev Scient Instrum 1986;57:655–7.
[7] White FM. Fluid mechanics. Boston: McGraw-Hill Book Company; 2003.
[8] Donnelly RJ, Barenghi CF. The observed properties of liquid helium at the saturated vapor pressure. J Phys Chem Ref Data 1998;27:1217–74.
[9] Bradley PE, Radebaugh R. Properties of selected materials at cryogenic temperatures, Technical Report, CRC Press Boca Raton, FL; 2013.
[10] Mann DB, Stewart R. Thermodynamic properties of helium at low temperatures and high pressures, volume 8, US Department of Commerce, Office of Technical Services; 1959.
[11] Arp VD, McCarty RD. Thermophysical properties of helium-4 from 0.8 to 1500 K with pressures to 2000 MPa; 1989.